Topics in Current Chemistry Collections

Xian-He Bu
Michael J. Zaworotko
Zhenjie Zhang *Editors*

Metal-Organic Framework

From Design to Applications

Springer

Topics in Current Chemistry Collections

Aims and Scope

The series *Topics in Current Chemistry Collections* presents critical reviews from the journal *Topics in Current Chemistry* organized in topical volumes. The scope of coverage is all areas of chemical science including the interfaces with related disciplines such as biology, medicine and materials science.

The goal of each thematic volume is to give the non-specialist reader, whether in academia or industry, a comprehensive insight into an area where new research is emerging which is of interest to a larger scientific audience.

Each review within the volume critically surveys one aspect of that topic and places it within the context of the volume as a whole. The most significant developments of the last 5 to 10 years are presented using selected examples to illustrate the principles discussed. The coverage is not intended to be an exhaustive summary of the field or include large quantities of data, but should rather be conceptual, concentrating on the methodological thinking that will allow the non-specialist reader to understand the information presented.

Contributions also offer an outlook on potential future developments in the field.

More information about this series at http://www.springer.com/series/14181

Xian-He Bu • Michael J. Zaworotko
Zhenjie Zhang
Editors

Metal-Organic Framework

From Design to Applications

With contributions from

Hongde An • Xian-He Bu • Sydney Butikofer • Ze Chang • Yao Chen
Peng Cheng • Guodong Ding • Wenjie Duan • Honghan Fei
Jia Gao • Shubo Geng • Leiduan Hao • Shengli Hou • He Huang
Matthew J. Hurlock • Sanjay Kumar • Tanay Kundu • Bin Li
Shengqian Ma • Jiyan Pei • Tony Pham • Binbin Qian
Guodong Qian • Xiaohang Qiu • Sahar Rajeh • Alexander Schoedel
Bhuvan B. Shah • Kai Shao • Ying Shi • Brian Space • Gaurav Verma
Hui-Min Wen • Bin Zhao • Dan Zhao • Zhengfeng Zhao
Guiyang Zhang • Ling Zhang • Qiang Zhang • Zhenjie Zhang

Springer

Editors
Xian-He Bu
College of Materials Science
and Engineering
Nankai University
Tianjin, China

Zhenjie Zhang
College of Chemistry
Nankai University
Tianjin, China

Michael J. Zaworotko
Department of Chemical Sciences
and Bernal Institute
University of Limerick
Limerick, Ireland

Partly previously published in Topics in Current Chemistry Volume 377 (2019); Topics in Current Chemistry Volume 378 (2020).

ISSN 2367-4067
Topics in Current Chemistry Collections
ISBN 978-3-030-47339-6

This Springer imprint is published by the registered company Springer Nature Switzerland AG
The registered company address is: Gewerbestrasse 11, 6330 Cham, Switzerland

Contents

Preface

We are now in the "Age of Gas" means that energy efficient approaches for gas purification and storage must be developed in order to further enable the utility of gases as fuels, therapies or feedstock chemicals. Porous solids such as zeolites and activated carbons are already used industrially in this context but they are ill-suited for many separation and storage applications, especially those that require ultra-high selectivity or extra-large surface area. These limitations are at least partly due to their narrow range of composition and difficulties with respect to design of pore size and/or pore chemistry. In short, it is difficult to fine-tune the properties of zeolites and activated carbons for a particular application. Fortunately, several new families of porous materials have emerged in the past two decades. These families are exemplified by a class of porous coordination networks known as metal-organic frameworks (MOFs), which are the subject of this topical collection.

MOFs are typically comprised of a metal or metal cluster (the "node") that is coordinated to a multi-functional organic ligand(s) (the "linker"). It is now well recognized that MOFs represent a new frontier in materials science because the "node and linker" approach to their design has afforded materials with the following features: unprecedented levels of permanent porosity; crystallinity that brings uniformity, process scale-up and reproducibility; modular compositions that can offer control over both structure and properties. This combination of features makes it unsurprising that MOFs have captured the imagination of chemists worldwide and they are primed to solve societal challenges in the areas of energy sustainability and environmental remediation. Today there are already tens of thousands of MOFs so the challenge is no longer how to make them. Rather, it is how to customize MOFs for a given application. As detailed below, the contributions in this topical collection are focused upon two main themes: design strategies for creation of new MOFs; structure-property relationships in MOFs in the context of topical applications of porous materials.

With respect to design strategies, there are three contributions herein. Rajeh & Schoedel discuss the use of metal oxide clusters as building blocks for functional MOFs. Duan & Chen et al., detail how to incorporate biomolecules into MOFs. The topic of interpenetration and how to control it is addressed by Verma and Ma et al..

The broad scope of properties that can be exhibited by MOFs is addressed in the remaining eight contributions. Qian and Bu et al. report on the switching properties of MOFs and how this phenomenon can be exploited for sensing and adsorption. Hao & Zhang et al. cover the use of MOFs for desulfurization of fuels. The uses of organosulfonate MOFs are presented and discussed by Zhang & Fei et al.. The application of molecular simulations to understanding and insight into the sorption properties of MOFs is detailed by Pham and Space. Gao and Zhang et al. summarized the progress on theoretical exploration and electronic applications of conductive 2-dimentional MOFs. Li & Qian et al. address hydrocarbon separations using MOFs whereas Shah and Zhao et al. present a review on the mechanochemical properties of MOFs. The final contribution by Shi & Zhao et al. covers the use of MOFs for catalytic conversions of CO_2.

This topical collection highlights the two key reasons that interest in MOFs has grown exponentially to the point where there are over 5000 publications annually. The modularity of MOFs, which makes them amenable to systematic study of structure-function relationships, also allows chemists to exert control over pore size and pore chemistry in a way that is not possible in existing classes of porous materials. The outcome of such control is unprecedented properties and performance as detailed herein.

Xian-He Bu
College of Materials Science and Engineering,
Nankai University, Tianjin, China

Michael J. Zaworotko
Department of Chemical Sciences and Bernal Institute,
University of Limerick, Limerick, Ireland

Zhenjie Zhang
College of Chemistry, Nankai University,
Tianjin, China

Topics in Current Chemistry (2020) 378:19
https://doi.org/10.1007/s41061-020-0281-0

REVIEW

Why Design Matters: From Decorated Metal Oxide Clusters to Functional Metal–Organic Frameworks

Alexander Schoedel[1] · **Sahar Rajeh**[1]

Received: 30 June 2019 / Accepted: 14 January 2020 / Published online: 3 February 2020

Abstract

The opportunity to generate functional solids with defined properties by deliberate design has not been materialized in traditional solid-state chemistry over many decades. The emergence of metal–organic frameworks (MOFs), permanently porous, crystalline solids with defined metrics, has allowed for studying design, synthesis, and properties, which then translated into new applications. Aggregates of metal ions stitched together by multidentate functional groups form such metal oxide clusters and represent the nodes of MOFs. These clusters, termed secondary building units (SBUs), are decorated with organic moieties that provide directionality and can be linked through geometric principles into extended nets using organic molecules (spacers). This concept of reticular chemistry has afforded permanently porous MOFs, and has resulted in over 20,000 structures over the past 20 years. However, there are still only a limited number of symmetric, discrete SBUs commonly used to design and synthesize MOFs. We herein introduce the most important SBUs that have emerged over time together with prototypal MOF structures and their fundamental applications. Both the discovery and the scientific impact will be highlighted alongside advantages and/or drawbacks. In addition, an outlook will be given on how the combination of multiple SBUs can lead to heterogeneous but ordered materials with higher complexity and functionality.

Keywords Metal-oxide clusters · Secondary building units · Framework design · Reticular chemistry · Topology

Chapter 1 was originally published as Schoedel, A. & Rajeh, S. Topics in Current Chemistry (2020) 378: 19. https://doi.org/10.1007/s41061-020-0281-0.

✉ Alexander Schoedel
aschoedel@fit.edu

[1] Department of Biomedical and Chemical Engineering and Sciences, Florida Institute of Technology, 150 W University Blvd, Melbourne, FL 32901, USA

1 Introduction

> "One of the continuing scandals in the physical sciences is that it remains in general impossible to predict the structure of even the simplest crystalline solids from a knowledge of their chemical composition"
> (John Maddox,1988) [1].

In this statement, Sir John Maddox, then the editor of *Nature*, referred to the enormous challenges of achieving structures by design associated with solid-state materials in general. Only 1 year later, Hoskins and Robson detailed the first example of deliberately designed and synthesized frameworks using geometrically defined building units [2]. A combination of tetrahedral Cu^{I} centers together with rigid organic nitrile linkers enabled the prediction and synthesis of a diamond (**dia**) net.

Although, metal–organic crystals composed of single metal ion units, i.e., $Cu(–CN)_4$ and dinitrile linkers were discovered in earnest in the late 1950s, their enormous potential has long remained unnoticed [3–5]. Those and related 1D, 2D, and 3D nets were later termed coordination polymers and enabled characterization at the atomic level by means of single-crystal X-ray diffraction. During the 1990s, other coordination polymers emerged, mainly built from single metal ions and linear pyridyl linkers, e.g., 4,4′-bipyridine. In these cases, interpenetration has often precluded the formation of cavities and the establishment of permanent porosity. However, these sometimes-called "first-generation" metal–organic frameworks (MOFs) have set the groundwork for development of more robust and complex materials. Nonetheless, metal–pyridine-based frameworks still represent a very active research area today, particularly with respect to gas adsorption and separation applications [6, 7].

Metal–organic frameworks (MOFs) have since attracted considerable scientific interest due to their many potential applications, such as gas storage and separation, catalysis, and chemical sensing, among others. Their potential impact on environmental issues in energy-related fields holds great promise towards carbon-neutral cycles, including the sequestration of carbon dioxide or the storage of methane and hydrogen for vehicular applications [8]. MOFs are composed of metal cluster entities, often referred to as secondary building units (SBUs) [9], that are in turn joined with multifunctional, branched organic molecules, the linkers. The inorganic and organic units are connected into extended, porous structures by virtue of crystal engineering [10] or reticular chemistry [11]. These concepts provide many opportunities for making robust metal–organic crystals by design and for translating molecular functionality and reactivity into the solid state [12]; this is in contrast to inorganic zeolites [13], mesoporous silica [14], and porous carbon [15] that are useful materials because of their permanent porosity and architectural stability, but lack of a modular nature and the amenability to fine-tuning of properties.

Herein, we focus on what is referred to as "second-generation MOFs." They are composed of discrete high-symmetry metal–carboxylate clusters, the SBUs.

Their architectural stability allows for the evacuation of guests from the cavities or channels to create permanently porous materials. The difference to metal–pyridine coordination polymers arises from the bond energy between the building units, i.e., the neutral M–N bond compared to the charged M–carboxylate bond. However, the bond energy is still low enough to enable reversible reactions and therefore the growth of single crystals [16]. Metal–carboxylate MOFs had gained traction by the end of the 1990s following seminal contributions by Yaghi, Williams, and Kitagawa [17–19]. The first report on a microporous (pore diameter <2.0 nm) material, termed MOF-2, established the determination of surface area and pore volume. After synthesis, the solvent molecules were removed and reversible type I gas sorption isotherms (N_2, 77 K) were collected. This method has since become the gold standard for proof of porosity.

2 Secondary Building Units

High-symmetry building units allow exquisite control over the coordination environment, which makes them highly desirable for the rational design of new nets. Although there are many different carboxylate-decorated clusters reported as discrete entities [20], only a dozen or so have thus far been utilized in the construction of MOFs.

In this contribution, we highlight some of the "classic" SBUs that were developed relatively early, such as basic zinc acetate $Zn_4O(–COO)_6$, square paddlewheel $Cu_2(–COO)_4$, and trigonal prismatic $M_3O(–COO)_6$ clusters (Fig. 1). Recently, new MOFs from these building units were developed by using the "heterogeneity within order" concept, the introduction of more than two metal ions and/or linkers to synthesize materials of greater complexity. These MOFs were able to surpass the performance of binary (one metal ion, one linker) counterparts in terms of gas adsorption capacity [21]. We then emphasize newer building units that have gained momentum a few years ago, such as $Zr_6O_4(OH)_4(–COO)_{12}$, ring-like SBUs $Al_8(OH)_8(–COO)_{16}$, $UO_2(–COO)_3$, or rare earth metal clusters. Each of their geometries translates to highly stable architectures and some provide additional opportunity for linker installation. Such cluster entities produce valuable MOF platforms for many applications by addressing the drawbacks of the "classic" SBUs.

3 Topology and Points of Extension

Knowledge about the topology of MOFs provides fast opportunity for designed synthesis. Reticular chemistry is concerned with the simplification of MOF structures by deconstructing them into their underlying nets, i.e., the atoms are the vertices (or nodes) and are linked together by the bonds (or edges). Embeddings of nets are collected in a searchable online database, the Reticular Chemistry Structure Resource (RCSR) [22]. They are assigned three-letter, lowercase, bold symbols in the format **xyz**. The symbols may have an extension as in **xyz-a**. For example, in the diamond

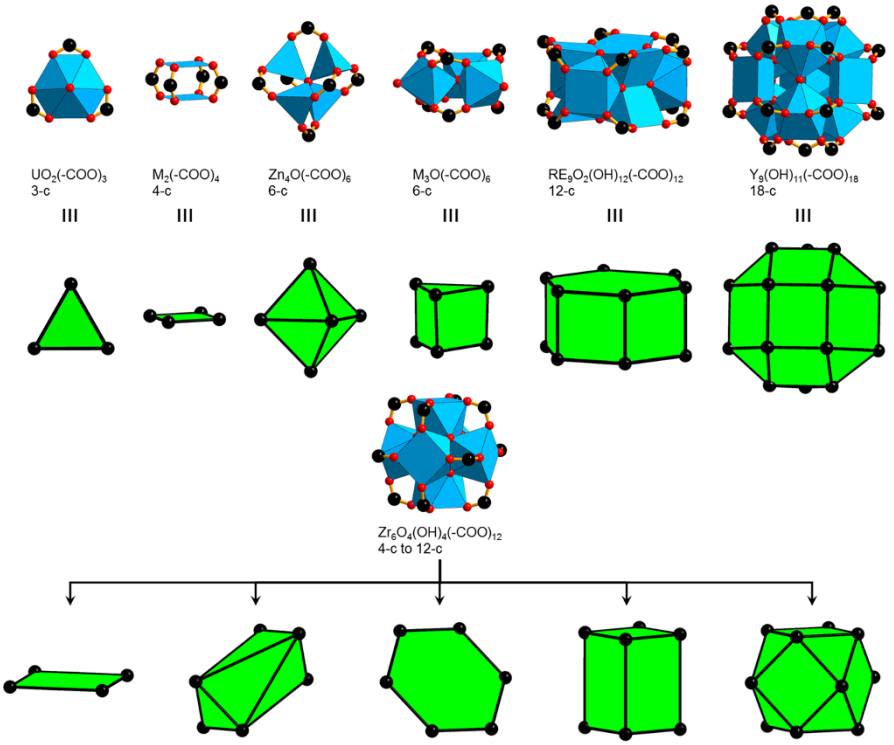

Fig. 1 Common secondary building units (SBUs) to construct MOFs. Color code: black, C; red, O; blue polyhedra, metal

(**dia**) structure, each carbon atom represents a tetrahedral vertex and the C–C bonds are the edges. The vertices in MOFs with multiatom SBUs are usually their barycenter while the organic linker serves as the edge.

Herein, we classify the presented SBUs by their points of extension (POE) which reflects the number of possible connections between one metal cluster and other metal clusters through organic linkers [20]. Regardless of the MOFs, the pattern of POE defines the shape of the metal cluster SBU. The proper assignment of POE in

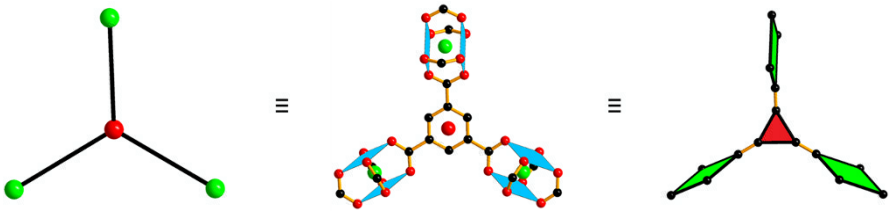

Fig. 2 Deconstruction approach of HKUST-1. $Cu_2(–COO)_4$ and BTC represent square planar and triangular shaped SBUs, respectively. Color code: black, C; red, O; blue polyhedra, Cu. Hydrogen atoms are omitted for clarity

metal–carboxylate frameworks is always the carboxylate C-atom. For example, the $Cu_2(–COO)_4$ cluster, which forms HKUST-1, contains four carboxylate carbons that serve as POE in a square planar shaped SBU (Fig. 2). Simplification renders it into a 4-c node. The tritopic BTC moiety (H_3BTC = 1,3,5-benzene tricarboxylic acid) corresponds to a 3-c node. Therefore, the topology of the resulting (3,4)-c net is **tbo** (twisted boracite). The notation -c stands for coordination of the particular cluster and should not be confused with connection. Many times, the augmented version of the net, here **tbo-a**, is represented by replacing the nodes by coordination figures (4-c squares and 3-c triangles).

The minimum number of POE is 3, a triangular shaped SBU, and the maximum is 18, an **eto** polyhedron. We would like to point out that polyhedral building units also exist, e.g., the 24-c nanoball in the (3,24)-c **rht**. Since those and related nets can be further deconstructed into a trinodal (3,4)-c **ntt** net, we exclude them purposely from this review [23]. Each of the building units will be presented together with a different MOF that is considered prototypal for an isoreticular (of the same net topology) class of MOFs [24]. However, there is a distinction between prototypes and default nets, the latter resulting only from linear connection of SBUs. In contrast, the prototypes discussed herein have often spurred interest in a particular net topology, which in turn led to very active research. We also emphasize the design aspects, and how to achieve fine-tuning of structure–property relationships. Current benchmark materials are also highlighted together with potential or actual applications.

4 Three Points of Extension

We introduce how SBUs with 3-c can give various MOFs designs based on a triangular shaped SBU with different topologies by changing linker geometries (Fig. 3).

Commonly, uranium(VI) exists as a linear uranyl cation $[UO_2]^{2+}$ that shows additional coordination in the equatorial plane to generate tetragonal, pentagonal, and hexagonal bipyramidal geometries. Its existence is long and well known; however, the first uranyl coordination compound containing three carboxylates in a hexagonal bipyramidal geometry was first reported in the mid-1930s [25]. Some coordination polymers composed of $UO_2(–COO)_3$ together with flexible linkers were reported earlier, however, the default net for 3-c $UO_2(–COO)_3$ SBUs, $(UO_2)_2(BDC)_3$ (H_2BDC = 1,4-benzenedicarboxylic acid, Fig. 3) was first obtained in 2006 [26]. The compound was synthesized in hydrothermal reactions at relatively high temperatures producing a 2D 3-c **hcb** with a twofold interpenetration. Two ammonium cations per formula unit balance the negative charge. It was also shown that bulkier linkers, such as 1,4-NDC (1,4-H_2NDC = 1,4-naphthalenedicarboxylic acid) can be used to avoid interpenetration.

If uranyl nitrate is reacted with DMF (*N*,*N*-dimethylformamide) together with H_3BTB (H_3BTB = 4,4′,4″-benzene-1,3,5-triyl-tribenzoate) a framework of formula $(UO_2)BTB$ is produced [27]. It shows the same 3-c **hcb** topology as the previously described framework; however, the BTB linker represents half of the nodes. Desymmetrization of BTB by introducing DCPB (H_3DCPB = 3,5-di(4′-carboxylphenyl)

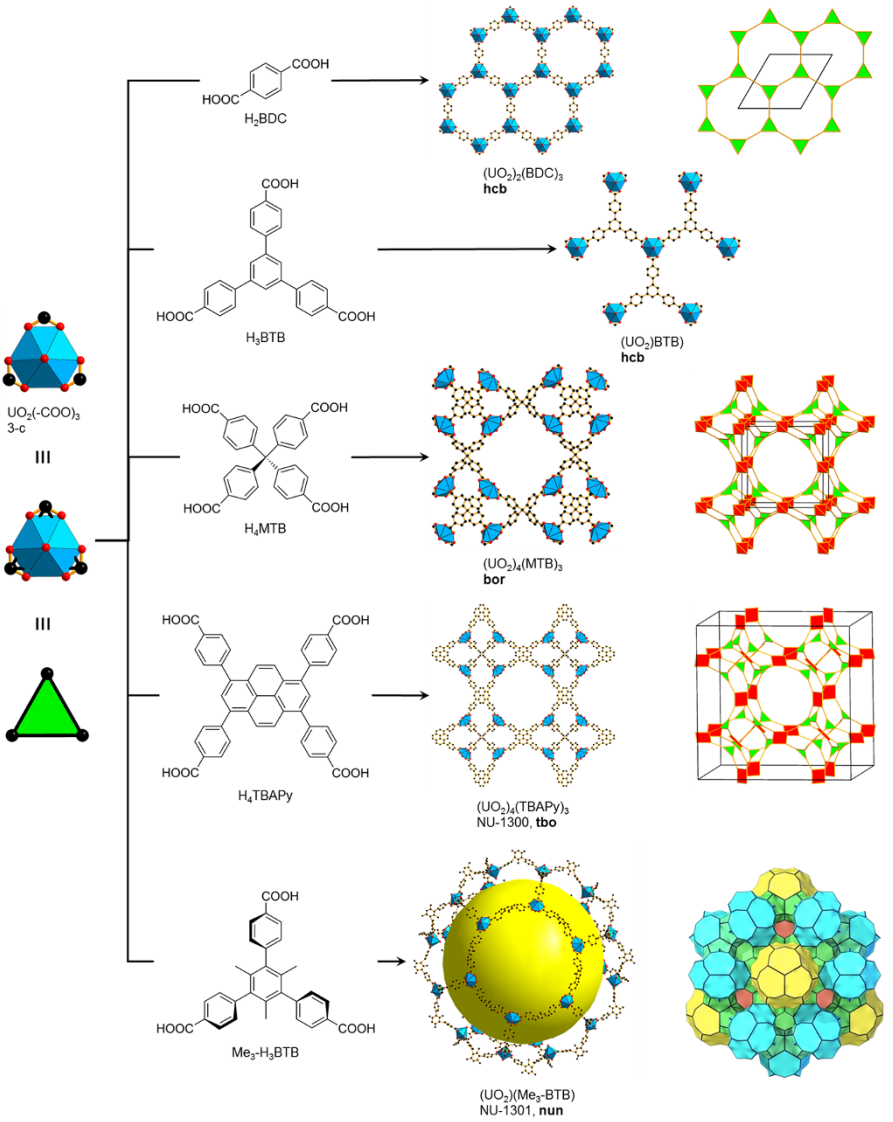

Fig. 3 MOFs constructed from 3-c $UO_2(–COO)_3$ SBUs and various linkers. Color code: black, C; red, O; blue polyhedra, U. The yellow spheres represent the empty space in the framework. Hydrogen atoms and interpenetrated nets are omitted for clarity

benzoic acid) causes significant distortion which in turn leads to a threefold interpenetrated **hcb** net. 3D porous crystals were produced, which show an apparent BET (Brunauer–Emmett–Teller) area of 924 $m^2\ g^{-1}$ (N_2, 77 K). Moreover, the charge-balancing DMA cations (dimethylammonium) were exchangeable, allowing for selective removal of cesium from aqueous solutions. The selectivity was determined against other alkali and some alkaline earth metal cations.

When 3-c $UO_2(–COO)_3$ SBUs are connected together via the tetrahedral carboxylate linkers MTB (H_4MTB = tetrakis(4-carboxyphenyl)methane), two structures of formula $(UO_2)_4(MTB)_3$ were produced [28]. They show different (3,4)-c topologies based on triangles and tetrahedra, **bor** (Fig. 3) and **ctn**, respectively. While the **ctn** net is non-interpenetrated, the **bor** net shows a twofold interpenetration. The difference in topology was explained by the distortion of the tetrahedral linker that may occur when the reaction conditions change. Adsorption of organic dyes into the frameworks was reported; however, no gas adsorption was conducted and no BET surface area was determined. Recently, a tetrahedral silicon-containing linker has produced a twofold interpenetrated framework with the same (3,4)-c **bor** topology [29].

If methyl-functionalized BTB, Me_3-BTB is linked together with $UO_2(–COO)_3$, a framework with formula $(UO_2)(Me_3\text{-BTB})$ is produced [30]. The methyl groups cause a distortion in the benzoate moieties being orthogonal to the central phenyl ring. Therefore, the default 2D 3-c **hcb** topology is impossible, and depending on the angle formed, 3-c **ths-b** (90°) or 3-c **srs-b** (< 90°) topologies would be expected. Nevertheless, the MOF termed NU-1301 shows a previously unreported 17-nodal 3-c **nun** topology. It crystallizes in a 173.3-Å cubic unit cell, the largest thus far for nonbiological materials. The unprecedented complexity of the structure generates internal cavities of 5.0 and 6.2 nm in diameter. With a density of only 0.124 g cm^{-3} it represents the lowest density MOF reported to date, which is quite remarkable, given the heavy nature of the uranyl building unit. The apparent BET surface area (Ar, 87 K) was determined to be 4750 m^2 g^{-1}. It was also demonstrated that hydrophobicity can be adjusted by anion exchange. NU-1301 exemplifies that there are still many highly porous materials to be discovered, even by combination of relatively simple building units.

The combination of $UO_2(–COO)_3$ with a square planar, tetratopic linker TBAPy (H_4TBAPy = 1,3,6,8-tetrakis(*p*-benzoic acid)pyrene) produces a framework of formula $(UO_2)_4(TBAPy)_3$, named NU-1300 [31]. It shows the well-known (3,4)-c **tbo** topology, based on triangles and squares. The difference to an also possible (3,4)-c **bor** topology is the perfectly orthogonal benzoic moieties with respect to the pyrene core. NU-1300 contains two cages with diameters of 17 Å and 39 Å, together with interconnected cavities of 27 Å in diameter. After supercritical CO_2 activation, it revealed a BET surface area of 2100 m^2 g^{-1}. The authors showed that the anionic framework could effectively separate biological macromolecules as a result of their overall charge.

5 Four Points of Extension

Square paddlewheels of formula $M_2(–COO)_4$ (M = Cu, Zn) are the most commonly known MOFs that contain four POE. They can be joined with a wide range of multitopic linkers to produce a large diversity of functional frameworks. In particular, copper and zinc variants crystallize relatively easily under well-established reaction conditions, which then leads to predictable structures. We herein introduce seminal

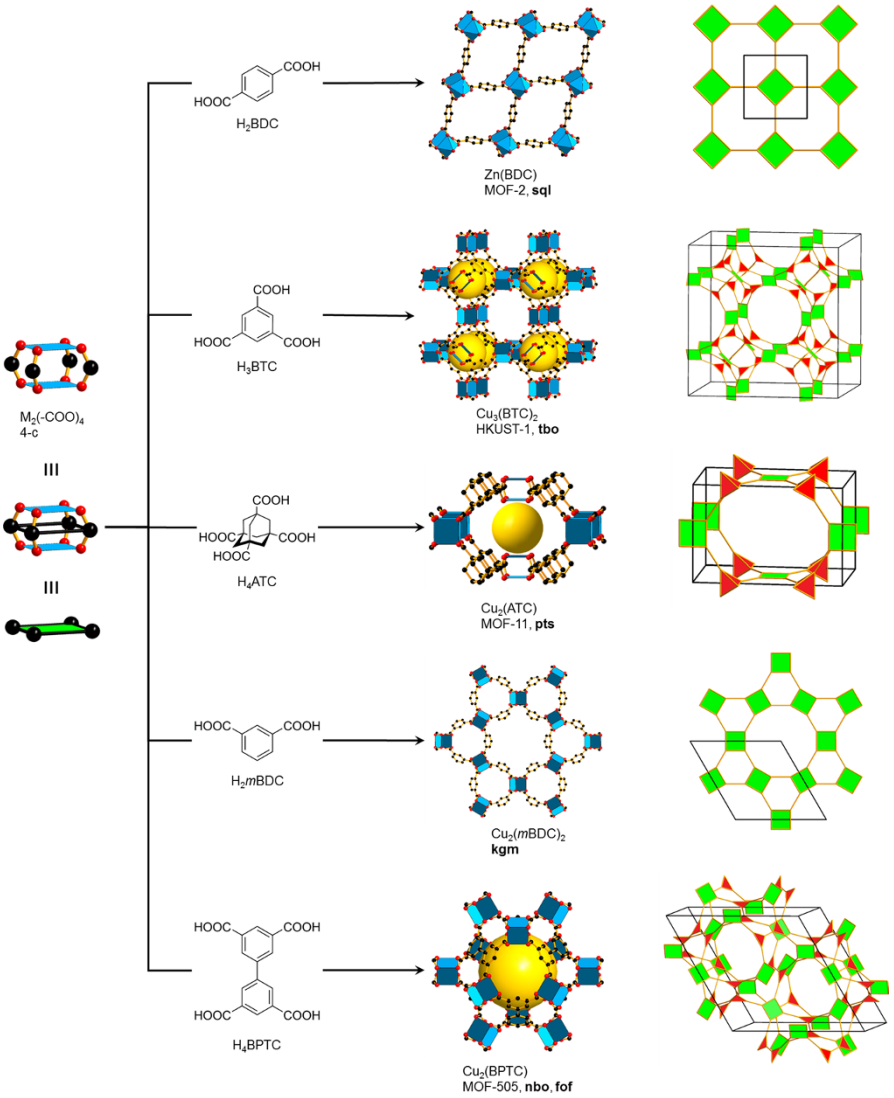

Fig. 4 MOFs based on the square paddlewheel SBU $M_2(–COO)_4$ and different linkers. Color code: black, C; red, O; blue polyhedra, Cu, Zn. The yellow spheres represent the empty space in the framework. Hydrogen atoms are omitted for clarity

MOFs that have been developed into families of frameworks or platforms and thus shaped the field towards the design of task-specific materials (Fig. 4).

MOF-2, $Zn(BDC)(H_2O)$ (H_2BDC = benzene-1,4-dicarboxylic acid) was first synthesized in 1998 and is built from $Zn_2(–COO)_4$ paddlewheel building units [17]. When linked with linear, ditopic BDC, the default, 2D square-grid net, 4-c **sql** was produced. MOF-2 gains additional stability through strong hydrogen-bonding interactions between the layers. This framework deserves special

attention since the first gas adsorption measurements using N_2 at 77 K have revealed its microporosity with a Langmuir surface area of 270 $m^2\ g^{-1}$, as well as a micropore volume of 0.10 $cm^3\ cm^{-3}$ (0.094 $cm^3\ g^{-1}$). This discovery represented a turning point in the MOF field towards carboxylate-based clusters as rigid and directional building units, leading to architecturally stable, permanently porous frameworks.

HKUST-1 (or MOF-199) is a renowned material built from $Cu_2(–COO)_4$ linked to tritopic BTC (H_3BTC = benzene-1,3,5-tricarboxylic acid) [18]. $Cu_3(BTC)_2$ crystallizes in a cubic structure with the (3,4)-c **tbo** topology. HKUST-1 was the first 3D MOF containing copper paddlewheel SBUs. It is prototypical and easy to make under many different conditions. The BET surface area after full activation is around 1800 $m^2\ g^{-1}$. Many variants of HKUST-1 were synthesized, including the use of different metal cations and the synthesis of isoreticular variants by using longer linkers. MOF-399 of formula $Cu_3(BBC)_2$ (H_3BBC = 4,4′,4″-(benzene-1,3,5-triyl-tris(benzene-4,1-diyl))tribenzoic acid) has long been known for the lowest crystal density in MOFs (0.126 g cm^{-3}), until the recent discovery of NU-1301 [30, 32].

$Cu_2(ATC)$ (MOF-11, H_4ATC = adamantane-1,3,5,7-tetracarboxylic acid) is built from $Cu_2(–COO)_4$ and tetratopic, tetrahedral-shaped ATC [33]. Thus, Linking of square and tetrahedral building units leads to binodal 4-c **pts** topology. Removal of the axial water molecules at the SBU of MOF-11 marks the discovery of open metal sites (OMS) in MOFs. Isoreticular frameworks were synthesized, such as H_4MTPC (4,4′,4″,4‴-methanetetrayltetrabenzoic acid) yielding $Cu_2(MTPC)$, and H_4MTBC (4,4′,4″,4‴-methanetetrayltetrabiphenyl-4-carboxylate) resulting in the twofold interpenetrated $Cu_2(MTBC)$ [34]. Both MOFs were activated for the first time through freeze-drying with benzene, showing a 300% and 30% improvement in BET surface area, when compared to regular activation procedures under vacuum.

In contrast to HKUST-1, the combination of $Cu_2(–COO)_4$ and an expanded triangular linker BTB produced $Cu_3(BTB)_2$ (MOF-14) with a (3,4)-c **pto** topology [35]. While triangles and squares in the (3,4)-c **tbo** net are coplanar, they are tilted with respect to each other in the **pto** net. It is the direct consequence of the steric hindrance between hydrogen atoms at the adjacent phenylene rings. The large pore size in MOF-14 enabled a twofold interpenetration, creating a periodic minimal surface. A Langmuir surface area of 1502 $m^2\ g^{-1}$ was estimated together with a pore volume of 0.53 $cm^3\ g^{-1}$ (N_2, 77 K).

Other examples in which geometric requirements of the linkers determine the topology of the resulting MOFs were observed in the first 4-c NbO (**nbo**) structure type framework $Cu_2(Br\text{-}BDC)_2$ (MOF-101) [36]. The combination of a $Cu_2(–COO)_4$ with 2-Br-BDC generates a 90° angle between the normally coplanar carboxylate groups and thus leads to an **nbo** instead of **sql** (MOF-2) topology. Variation of this angle in different organic linkers, and thus changing geometric requirements, enabled the synthesis of 0D, 2D, and 3D structures, by linking square paddlewheel SBUs [37]. These 0D and 2D structures are the underlying topologies for many 3D structures described in this review, and are therefore a critical design element in the synthesis of new MOFs.

A 2D structure composed of $Cu_2(–COO)_4$ and *m*BDC was synthesized, showing the topology of a nanoscale 4-c **kgm** lattice (Fig. 4) [38]. Such layers can be

linked through the 5-position of *m*BDC, therefore opening the possibility for many 3D frameworks. The parent compound, MOF-505, was first synthesized in 2005 and can be viewed as staggered **kgm** layers linked together, using BPTC (H_3BPTC = 3,3′,5,5′-biphenyltetracarboxylic acid) [39]. The topology was determined to be 4-c **nbo**, a combination of squares; however, the linker asymmetry would justify a deconstruction of BPTC into linked triangles. The deconstructed topology is 3,4-c **fof** [23]. Especially with respect to reticular chemistry approaches, it is crucial to recognize the **kgm** layers as a basis framework design. Since the discovery of MOF-505, many isoreticular frameworks with interesting properties have emerged. Very recently, MFM-102-NO_2 of formula $Cu_2((NO_2)_2$-QPTC) ($(NO_2)_2$-H_4QPTC = 2″,3′-dinitro-[1,1′:4′,1″:4″,1‴-quaterphenyl]-3,3‴,5,5‴-tetracarboxylic acid) was produced with a BET surface area of 2893 $m^2\ g^{-1}$ [40]. This framework shows optimal binding to acetylene molecules through a cooperative effect of Cu_2(–COO)$_4$ OMS together with –NO_2 groups. Therefore, its gravimetric acetylene adsorption at 1 bar and 298 K reaches 192 $cm^3\ g^{-1}$.

Linking of Cu_2(–COO)$_4$ with an angular *m*BDC (H_2*m*BDC = 1,3-benzenedicarboxylic acid) leads to a large structural diversity. A metal–organic polyhedron, termed MOP-1, Cu_{24}(*m*BDC)$_{24}$ consists of 12 paddlewheel units and 24 *m*BDC moieties with the shape of a truncated cuboctahedron [41]. These so-called nanoballs, which show in principle a 24-c **rco** topology, were used as the blueprint of many 3,24-c **rht** nets [42]. There is a review on the supramolecular building block (SBB) approach, which details linking of such 0D building blocks into 3D frameworks [43]. After discovery of the original **rht**-MOF-1 in 2008, functionalized and expanded hexacarboxylate linkers have led to isoreticular **rht** frameworks. A deconstruction approach suggested a derived trinodal (3,4)-c **ntt** to describe these frameworks [23]. The derived **ntt** net takes into account that both the nanoball and the threefold branch can be expanded to make isoreticular frameworks. An elegant example of fine-tuning the carbon dioxide adsorption properties was demonstrated in Cu_3(TPBTM) (H_6TPBTM = *N*,*N*′,*N*″-tris(isophthalyl)-1,3,5-benzenetricarboxamide), sometimes referred to as **rht**-amide [44]. This MOF exhibits an apparent BET surface area of 3160 $m^2\ g^{-1}$ and a pore volume of 1.27 $cm^3\ g^{-1}$. The functionalization with amide groups enhanced the CO_2 adsorption to 23.53 mmol g^{-1} at 298 K and pressures up to 20 bar. The heat of adsorption Q_{st} = 26.3 kJ mol^{-1} also increased significantly, compared to the unfunctionalized structure of PCN-61 [45]. The authors attribute this higher value to the large dipole moment of the amide groups as well as NH···OCO hydrogen bonds. Over the years, the hexatopic linker has continually been elongated, in particular to target ultrahigh surface area MOFs [46, 47]. For example, NU-110 contains a linker with an edge length of around 20 Å (Fig. 5) [48]. After activation of Cu_3(TCEPEPB) (H_6TCEPEPB = 1,3,5-tris[((1,3-carboxylic acid-5-(4-(ethynyl) phenyl))ethynyl)phenyl]benzene) with supercritical CO_2, gas adsorption measurements (N_2, 77 K) revealed a BET surface area of 7140 $m^2\ g^{-1}$ and a pore volume of 4.40 $cm^3\ g^{-1}$. NU-110 has long held both of these world records among porous materials.

A smaller type of MOP is obtained by decreasing the angle subtended at the dicarboxylates from 120° to 90° using H_2CDC (9*H*-carbazole-3,6-dicarboxylic acid) as a linker (Fig. 5). The obtained polyhedron Cu_{12}(CDC)$_{12}$ exhibits 12 POE

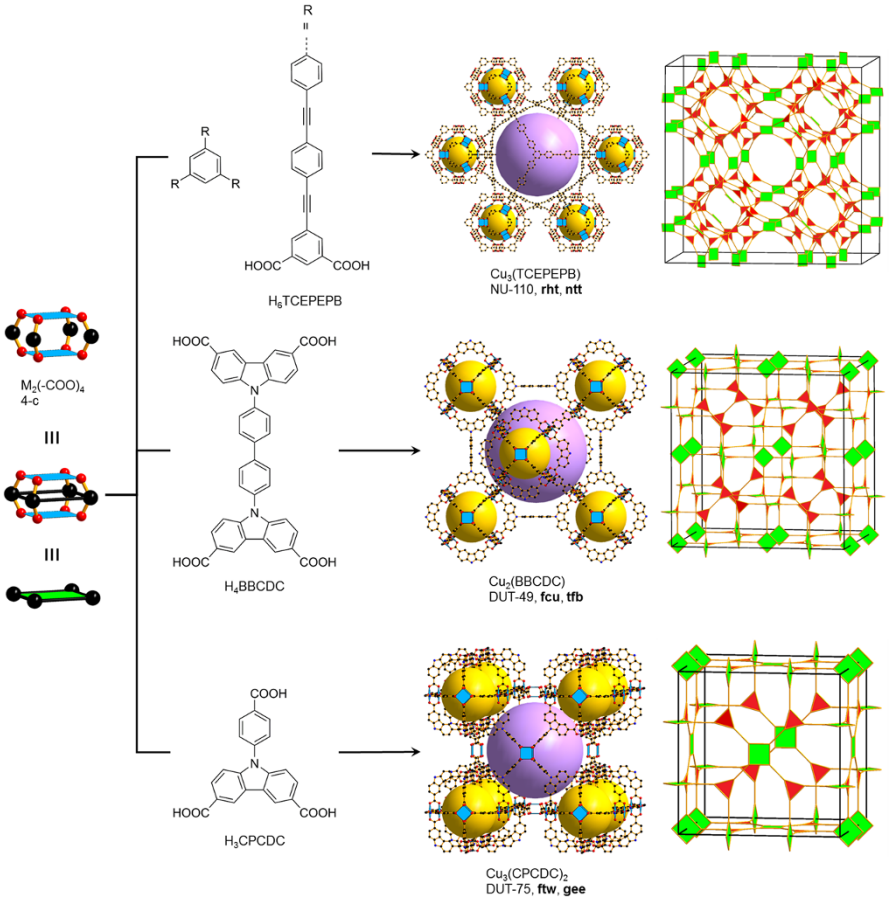

Fig. 5 MOFs based on 4-c square paddlewheel SBU $M_2(–COO)_4$ that generate linked $M_{24}(–m\text{BDC})_{24}$ **rco** MOPs (NU-110) or linked $M_{12}(–CDC)_{12}$ MOPs (DUT-49, DUT-75). Color code: black, C; red, O; blue polyhedra, Cu. The yellow and purple spheres represent the empty space in the framework. Hydrogen atoms are omitted for clarity

in a cuboctahedral (**cuo**) geometry, and an inner diameter of 12 Å [49]. It was further linked with a tetratopic BBCDC [H_4BBCDC = 9,9′-([1,1′-biphenyl]-4,4′-diyl) bis(9*H*-carbazole-3,6-dicarboxylic acid)] to produce DUT-49, Cu_2(BBCDC) [50]. The topology was determined as 12-c **fcu** if the **cuo** is considered as one 12-c building unit. As outlined for the **rht**-nets, it can also be deconstructed into a binodal (3,4)-c **tfb** net, taking into account the tetratopic nature of BBCDC. The **tfb** net also highlights the opportunity for reticular chemistry to change each edge length independently without alteration of the overall topology. Adsorption isotherms (N_2, 77 K) revealed a considerably high BET surface area of 5476 $m^2\ g^{-1}$ and a pore volume of 2.91 $cm^3\ g^{-1}$. Moreover, owing to its nearly optimal pore size, it shows a high gravimetric methane uptake of 308 mg g^{-1} at 110 bar and 298 K.

Recently, another CDC-containing linker was used to produce DUT-75 of formula $Cu_3(CPCDC)_2$ (H_3CPCDC = 9-(4-carboxyphenyl)-9*H*-carbazole-3,6-dicarboxylic acid) [51]. Similar topology determination revealed an overall 4,12-c **ftw** net. However, the deconstruction into the derived, trinodal (3,4)-c **gee** net is more suitable for reticular chemistry approaches. DUT-75 and its isoreticular expanded variant DUT-76 display very high BET surface areas of 4081 $m^2\ g^{-1}$ and 6344 $m^2\ g^{-1}$, respectively. They also demonstrate exceptional performance with respect to storage of methane and ethylene.

A polymorphic framework $Cu_2(mBDC)_2$ forms a 2D 4-c **sql** net (Fig. 6) [52]. The difference to **kgm** is the angles subtended at $Cu_2(–COO)_4$. Similar to **kgm** nets, **sql** nets can also be pillared through the 5-position of the *m*BDC. In 2011, an octatopic linker MTTBPDC

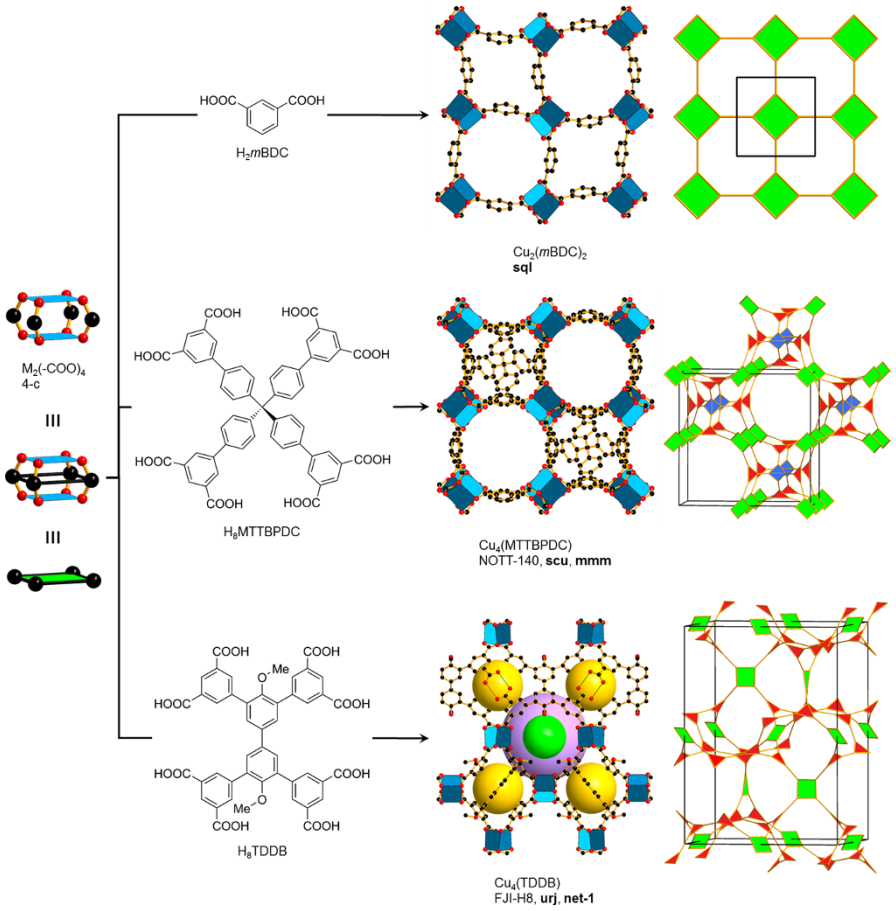

Fig. 6 MOFs based on the square paddlewheel SBU $M_2(–COO)_4$ that generates 4-c **sql** layers. Color code: black, C; red, O; blue polyhedra, Cu. The yellow, purple, and green spheres represent the empty space in the framework. Hydrogen atoms are omitted for clarity

[H_8MTTBPDC = 4′,4‴,4⁗,4⁗⁗,4⁗⁗⁗-methanetetrayltetrakis(([1,1′-biphenyl]-3,5-dicarboxylic acid)] was reacted with $Cu_2(–COO)_4$ to produce Cu_4(MTTBPDC), NOTT-140 [53]. The topology was reported as (4,8)-c **scu**, considering MTTBPDC as a single 8-c building unit. We believe that this might be an oversimplification, and instead should be regarded as a tetrahedron linked to four triangles [54]. The derived topology is the trinodal (3,4)-c **mmm**. This description considers the pillaring of **sql** nets and enables reticular chemistry strategies. NOTT-140 shows an apparent BET surface area of 2620 $m^2\ g^{-1}$ using Ar at 87 K. It was also suggested that NOTT-140 is a promising candidate for high capacity volumetric CO_2 storage (314.6 $cm^3\ cm^{-3}$, 20 bar, 293 K), with a Q_{st} of 24.7 kJ mol^{-1}.

Very recently, an octatopic linker TDDB (H_8TDDB = 3,3′,5,5′-tetra(3,5-dicarboxyphenyl)-4,4′-dimethoxybiphenyl) with a different geometry was reacted with $Cu_2(–COO)_4$ to produce Cu_4(TDDB), termed FJI-H8 [55]. The topology was determined as trinodal (4,8)-c **urj**. The octatopic linkers were considered as 8-c, which renders the other two vertex figures into squares and tetrahedra, respectively. Since there are no tetrahedra in the structure, we deconstructed the linker into four linked triangles. Then, the overall topology shows a new 4-nodal (3,4)-c net, here termed **net-1** (Fig. 6). FIJ-H8 exhibits an apparent BET surface area of 2025 $m^2\ g^{-1}$, which is consistent with the theoretical surface area of 1907 $m^2\ g^{-1}$. Acetylene adsorption measurements revealed an uptake of 277 cm^3 STP g^{-1} at 273 K and 1 bar which is slightly lower than ZJU-5 (290 cm^3 STP g^{-1}), a functionalized **fof**-topology MOF [56]. However, FIJ-H8 exhibited the highest C_2H_2 uptake of any MOF at room temperature (295 K, 224 cm^3 STP g^{-1}).

Four-coordinated zirconium clusters emerged only recently and long after the discovery of the first 12-c building unit $Zr_6O_4(OH)_4(–COO)_{12}$, known to form UiO-66 [57]. In this SBU, the zirconium(IV) ions sit on the corners of an octahedron, bound to four μ_3-O and four μ_3-OH on the octahedron's faces. The 12 bidentate carboxylate groups bridge two Zr each and are located on the edges of the octahedron. All carboxylate carbons serve as POE and span an overall cuboctahedral building unit. In 2015, a similar cluster of formula $Zr_6(OH)_{12}(SO_4)_4(–COO)_4$ was connected with adipic acid (H_2BUDC = butane-1,4-dicarboxylic acid) to produce $Zr_6(OH)_{12}(SO_4)_4(BUDC)_2$, a 4-c **sql**-topology framework [58]. The carboxylate groups of BUDC occupy only 4 of the 12 edges on the Zr_6 octahedron, leading to a square planar geometry. One half of the remaining coordination sites are capped with bidentate sulfate anions to balance the positive charges; the other half is bound to water molecules.

Very recently, another 4-c cluster $Zr_6O_4(OH)_6(HCOO)_6(–COO)_4$ was reacted with TPTC (H_4TPTC = [1,1′:4′,1″]- terphenyl-3,3″,5,5″-tetracarboxylic acid) to produce $Zr_6O_4(OH)_6(HCOO)_6(TPTC)_4$, NU-1400, a 3D framework with rhombic shaped pores [59]. The topology of NU-1400 is reported as 4-c **lvt** which has predetermined to flexibility and is comparable to the 4-c **sra** topology present in the rod MOF MIL-53 [60]. Since the linker geometry is elongated, we prefer the deconstruction into two joint triangles. Thus the 4-c **lvt** is rendered into a (3,4)-c **lim** topology (Fig. 7). The authors have demonstrated the catalytic performance of NU-1400 in the hydrolysis of DMNP (dimethyl 4-nitrophenyl

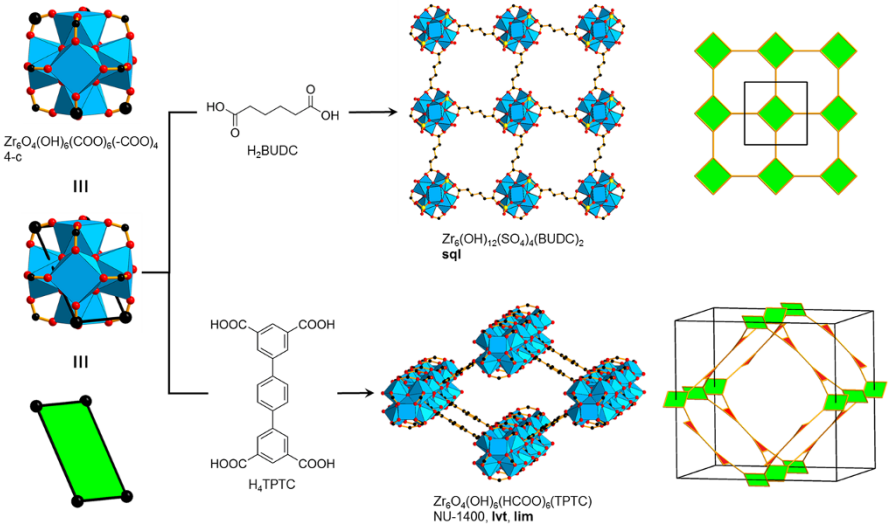

Fig. 7 MOFs based on a 4-c Zr_6-SBU capped with either sulfate or formate. Color code: black, C; red, O; yellow, S; blue polyhedra, Zr. Hydrogen atoms are omitted for clarity

phosphate), owing to the Lewis acidic zirconium(IV) sites. It was shown that the narrow-pore form showed only 30% conversion over the open-pore form with 90% conversion, opening up the opportunity to develop catalysts with adjustable accessibility.

6 Six Points of Extension

6.1 $Zn_4O(–COO)_6$: Octahedron

The first type of 6-c SBU $Zn_4O(–COO)_6$ has octahedral geometry and the structure of basic zinc acetate, which has been known as a molecular compound since the 1950s [61]. The cluster consists of a single O atom bound to four Zn^{2+} to form a Zn_4O tetrahedron. The edges of the tetrahedron are capped by carboxylates, where the carboxylate carbons, the POE, form the octahedron. Besides Zn, this structure has also been observed for Co and Be.

The first MOF $Zn_4O(BDC)_3$ containing this building unit was synthesized in the late 1990s and termed MOF-5 (Fig. 8) [62]. It shows 6-c **pcu** (primitive cubic) topology. Nitrogen gas adsorption (77 K) on MOF-5 revealed an estimated Langmuir surface area of 2900 $m^2\ g^{-1}$ and a pore volume of 1.04 $cm^3\ g^{-1}$. These values exceeded by far all known conventional porous materials such as zeolites, silicates, or porous carbon. Principles of reticular chemistry were applied to MOF-5 to produce a series of IRMOFs (isoreticular MOFs) for various applications, such as methane storage, among others [24]. In 2010, a "heterogeneity within order"

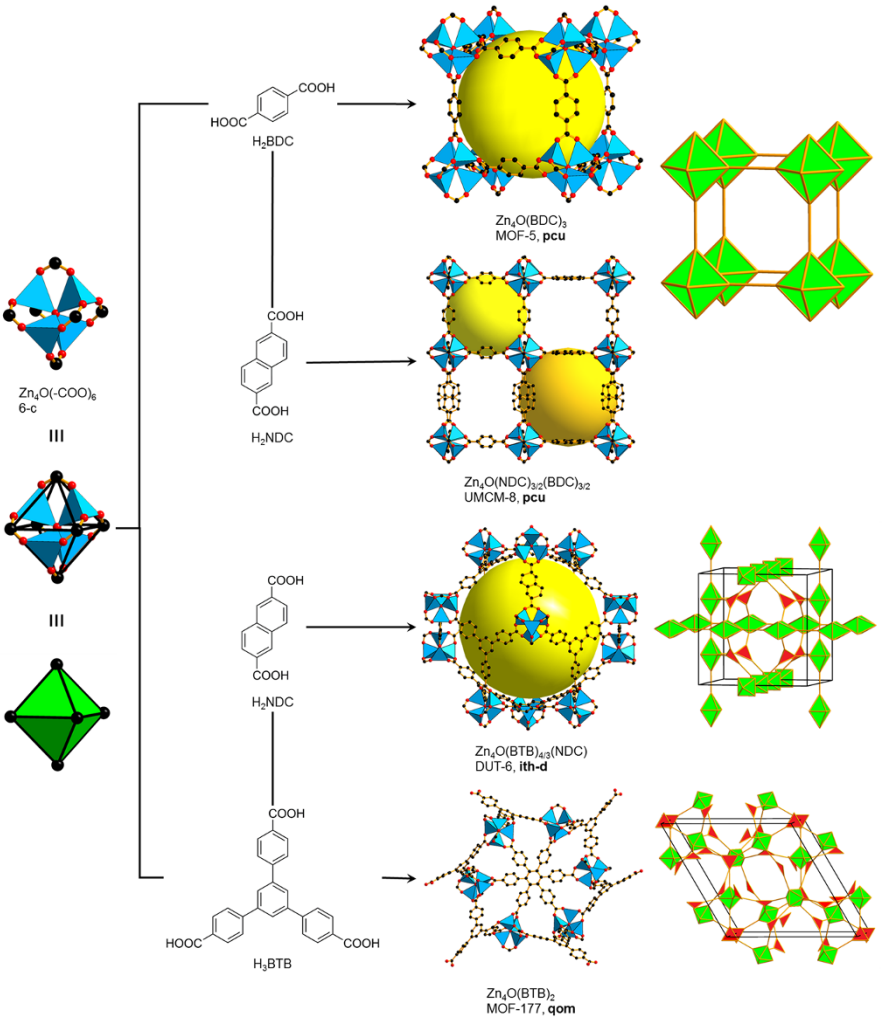

Fig. 8 MOFs constructed from 6-c $Zn_4O(–COO)_6$ SBUs. Color code: black, C; red, O; blue polyhedra, Zn. The yellow spheres represent the empty space in the framework. Hydrogen atoms are omitted for clarity

approach produced multivariate MOF-5 structures using up to eight differently functionalized BDC linkers in one phase [21]. It was shown that the arrangement of functional groups led to properties that are not just the simple linear sums of those of the pure compounds. For example MTV-MOF-5-EHI (E = NO_2-BDC, H = $(C_3H_5O)_2$-BDC, I = $(BnO)_2$-BDC) showed a 400% better selectivity towards CO_2 compared to the selectivity of pure MOF-5.

At a certain linker length, interpenetration of **pcu**-topology frameworks can be detrimental to achieving high surface area materials [24]. Therefore, another strategy was developed in 2012, using a combination of $Zn_4O(–COO)_6$

SBUs and mixed linkers of different length, such as H_2BDC, 1,4-H_2NDC, and H_2BPDC (4,4-biphenyldicarboxylic acid) [63]. The two new MOFs of formula $Zn_4O(NDC)_{3/2}(BDC)_{3/2}$ (UMCM-8) and $Zn_4O(NDC)_{3/2}(BPDC)_{3/2}$ (UMCM-9) show non-interpenetrated frameworks and apparent BET surface areas of 4030 $m^2\ g^{-1}$ and 4970 $m^2\ g^{-1}$, respectively (Fig. 8). In comparison, the BET surface area of MOF-5 is 3530 $m^2\ g^{-1}$ [64]. The authors particularly highlight the cost argument associated with such high porosity MOFs made from inexpensive, commercially available linkers.

In 2004, a new design approach to very high surface areas was introduced to produce the highly porous $Zn_4O(BTB)_2$, MOF-177 (Fig. 8) [65]. The topology consists of linked octahedra and triangles in a 5-nodal (3,6)-c **qom** net. The **qom** topology is recognized as superior over the other possible **rtl** (rutile) and **pyr** (pyrite) nets, since **qom** is not self-dual and interpenetration is inherently precluded. MOF-177 exhibits a Langmuir surface area of 4500 $m^2\ g^{-1}$ and a pore volume of 1.59 $cm^3\ g^{-1}$, using N_2 at 77 K. In 2010, a reticular chemistry approach using elongated triangular linkers produced the isoreticular structures $Zn_4O(BTE)_2$ (MOF-180, H_3BTE = 4,4′,4″-[benzene-1,3,5-triyl-tris(ethyne-2,1-diyl)]tribenzoate) and $Zn_4O(BBC)_2$ (MOF-200, H_3BBC = 4,4′,4,4″-[benzene-1,3,5-triyl-tris(benzene-4,1-diyl)]tribenzoate) which are also **qom** nets [66]. In such capacity, MOF-200 shows a high apparent BET surface area of 4530 $m^2\ g^{-1}$. In addition to isoreticular expansion, the use of mixed linkers—a linear (H_2BPDC) and a triangular (H_3BTE)—enabled the synthesis of MOF-210 with **toz** topology. At the time of its synthesis, this material held the world record in BET area with a value of 6240 $m^2\ g^{-1}$. It also exhibits a pore volume of 3.60 $cm^3\ g^{-1}$. Up until today, MOF-210 represents the only **toz** topology reported.

Another mixed linker platform is **ith-d**-topology MOFs, with DUT-6 (MOF-205) as the parent compound (Fig. 8) [66, 67]. Both tritopic H_3BTB and ditopic H_2NDC were combined with octahedral $Zn_4O(–COO)_6$ SBUs to produce $Zn_4O(BTB)_{4/3}(NDC)$. Each SBU is coordinated with four BTB and two NDC linkers. The **ith-d** topology is of great interest, since all tilings are 5-rings forming face-transitive dodecahedra and tetrahedra in a ratio of 1:3. MOF-205 shows an apparent BET surface area of 4460 $m^2\ g^{-1}$ and a pore volume of 2.16 $cm^3\ g^{-1}$. The **ith-d** topology served as a blueprint for many functional materials, including quaternary frameworks with programmed pore architectures and three different linkers. MUF-7a of formula $Zn_4O(BTB)_{4/3}(BDC)_{1/2}(BPDC)_{1/2}$ was synthesized in 2013 and exhibits an apparent BET surface area of 4140 $m^2\ g^{-1}$ and a pore volume of 1.94 $cm^3\ g^{-1}$ [68]. This MOF shows a high complexity, but compared to MTV-MOF-5, the different linkers are ordered and can be located with atomic precision. Very recently, an in silico design approach was applied for the synthesis of the ultrahigh porosity MOF DUT-60 [69]. Careful consideration of the **ith-d** topology enables the generation of large pores that are interconnected with "auxiliary" linkers to add robustness and avoid interpenetration. DUT-60, $Zn_4O(BBC)_{4/3}$(BCPBD), was produced by combination of $Zn_4O(–COO)_6$ with triangular H_3BBC and linear BCPBD (H_2BCPBD = 1,4-bis-*p*-carboxyphenylbuta-1,3-diene). It shows pores of diameter 37 Å and 15 Å, and has a crystal density of 0.187 g cm^{-3}, approaching those of the lowest density materials, MOF-399 and NU-1301 [30, 32]. Nitrogen

adsorption isotherms after supercritical CO_2 activation revealed an apparent BET surface area of 7839 $m^2\ g^{-1}$ and a pore volume of 5.02 $cm^3\ g^{-1}$, surpassing NU-110 (7140 $m^2\ g^{-1}$, 4.40 $cm^3\ g^{-1}$) [48]. Therefore, DUT-60 is the new world record holder in terms of surface area and pore volume among all porous materials.

Combination of the $Zn_4O(–COO)_6$ building unit together with a triangular $Cu_3(OH)(–PZ)_3$ produces **ott** (FDM-3), **umt** (FDM-6), and **ith-d** (FDM-7), and topology frameworks [70, 71]. Since these MOFs contain M–N coordination bonds, they are not discussed in detail.

6.2 $M_3O(–COO)_6$: Trigonal Prism

The other large class of 6-c nets relies on a very common cluster, the trigonal prism. It consists of a single μ_3-O bound to three $M^{2+/3+}$ to form a M_3O triangle. The four equatorial positions of each octahedron are capped by carboxylates, where the carboxylate carbons, the POE, form a trigonal prism. A water molecule or a charge-balancing hydroxide usually occupies the remaining coordination site. Basic chromium(III) acetate was first synthesized around 100 years ago and its absolute structure was elucidated by single-crystal X-ray diffraction in 1965 [72].

In 2002, the first 3D framework $V_3O(m\text{BDC})_3$, MIL-59, based on $V_3O(–COO)_6$ trigonal prismatic SBUs was reported (Fig. 9) [73]. It crystallizes in a 6-c **pcu**-topology net, which seems unusual, given the 120° angle in *m*BDC. However, this angle is compensated by the angle subtended at the trigonal prism. MIL-59 was later used as a blueprint in the development of In-**soc**-MOF, detailed below.

Linking of $M_3O(–COO)_6$ SBUs (M = Cr, Fe) was initially explored through the use of linear dicarboxylates, producing the MIL-88 series (MIL = Materials of Institute Lavoisier) as well as MOF-235 [74, 75]. In particular, three of these MOFs are special with respect to their properties and potential applications: MIL-88, MIL-100, and MIL-101 [76, 77]. MIL-100 and MIL-101 crystallize in a zeolitic **mtn**-topology framework and are not detailed it in this review since their framework design is not straightforward. The default net for linking trigonal prismatic nodes was first described in MOF-235 as 6-c **acs** [75]. The framework is identical to the later MIL-88B, with different guest molecules. The MIL-88 platform was produced by using different linkers such as H_2EDC (MIL-88A), H_2BDC (MIL-88B), H_2NDC (MIL-88C), and H_2BPDC (MIL-88D) [78]. All MOFs are isoreticular and they undergo large structural changes, also known as breathing, upon exposure to different guest molecules [79]. In the MIL-88 series, these reversible breathing phenomena reach high amplitudes of up to 270% of the original unit cell volume, without loss of crystallinity.

An elegant example of a MIL-101 polymorph, $Fe_3O(BDC)_3$, was recently reported with a binodal 6-c **flu-e** topology [80]. This structure was predicted in 2005 as MIL-hypo-2 and synthesized through a stepwise strategy using BDC and *m*PC (H*m*PC = pyridine-3-carboxylic acid (nicotinic acid)) [81]. The framework composed of rhombicuboctahedra possesses a large framework tension, which was mitigated in situ by capping half of the square windows with $Fe(m\text{PC})_4$. In MCF-37,

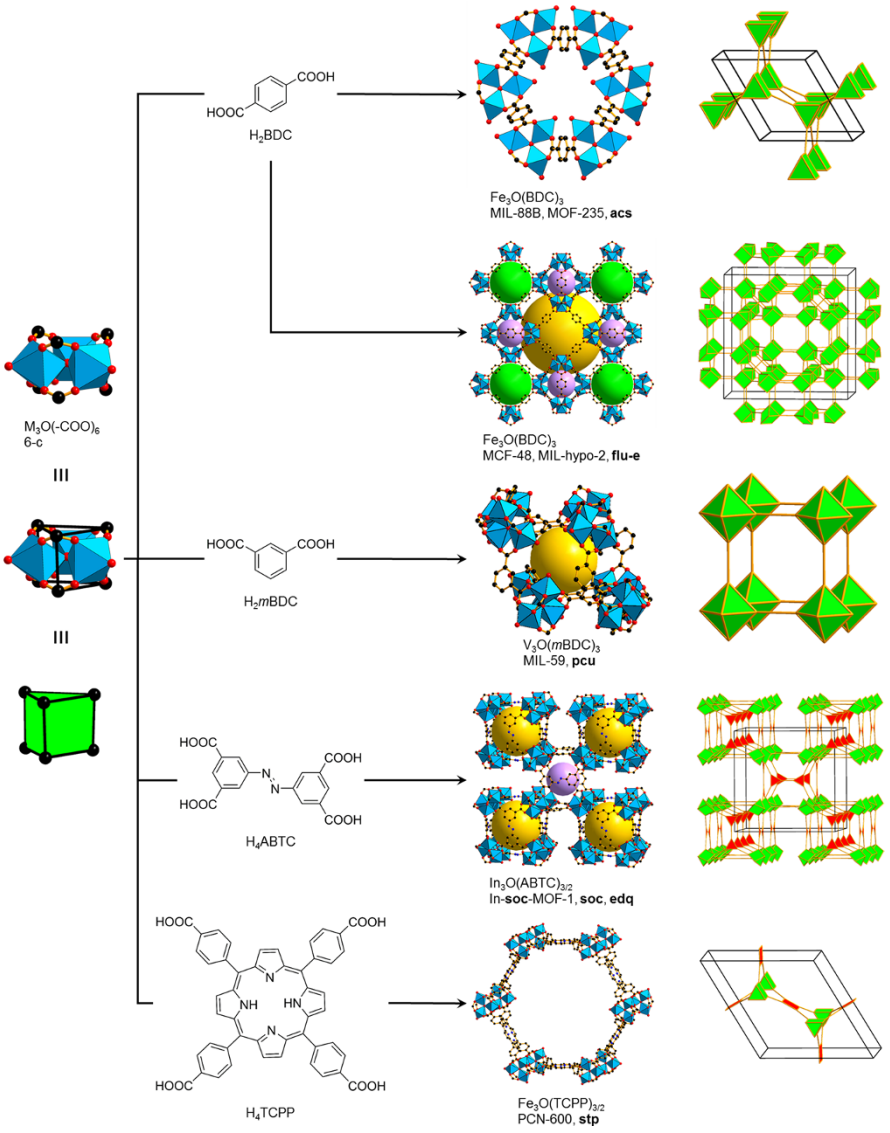

Fig. 9 MOFs formed by 6-c trigonal prismatic $M_3O(–COO)_6$ SBUs. Color code: black, C; red, O; blue polyhedra, metal. The yellow, purple, and green spheres represent the empty space in the framework. Hydrogen atoms are omitted for clarity

$[Fe_3O(BDC)_3]_4[Fe(mPC)_4]_3$, these complexes are coordinated to the OMS of the trigonal prismatic clusters to produce a new (4,9)-c net, herein termed **net-2**. After removal of the caps, the 6-c **flu-e**-topology framework, MCF-48, was obtained. Subsequently, cobalt paddlewheel units $Co_2(mPC)_4$ could be installed at the OMS in a postsynthetic process. The resulting MCF-49, $[Fe_3O(BDC)_3]_4[Co_2(mPC)_4]_3$, shows exceptional oxygen evolution reaction activities.

The first example of a (4,6)-c **soc**-topology MOF $In_3O(ABTC)_{3/2}$ (H_4ABTC = (*E*)-5,5′-(diazene-1,2-diyl)diisophthalic acid) was obtained in 2007 by combining tetratopic linkers with $In_3O(–COO)_6$ trigonal prisms [82]. This framework exhibits a surface area of 1400 $m^2\ g^{-1}$ and a high hydrogen uptake of 2.61 wt%, at 77 K. More importantly, the versatile structure has since led to many functional, isoreticular variants. It was shown that a mixed Fe-Co-**soc**-MOF, named PCN-250, shows exceptional stability in acid and base and a high methane deliverable in a 35–1 bar pressure swing adsorption [83]. In 2015, an isoreticular aluminum-containing framework termed Al-**soc**-MOF-1 $Al_3O(TCPT)_{3/2}$ (H_4TCPT = 3,3″,5,5″-tetrakis(4-carboxyphenyl)-*p*-terphenyl) was reported [84]. The longer TCPT linker can be deconstructed into two 3-c nodes, leading to a (3,6)-c **edq** topology [54]. Herein, the octahedral vertex figures of **soc** eventually become trigonal prismatic which is a better representation of the actual structure. The Langmuir surface area of Al-**soc**-MOF-1 is 6000 $m^2\ g^{-1}$ and the pore volume is 2 $cm^3\ g^{-1}$. High pressure gas adsorption of methane revealed the highest volumetric working capacity of 264 cm^3 (STP) cm^{-3} (5–80 bar, 258 K) among any porous material, fulfilling the DOE target at that time. In addition, a recently reported chromium(III) analogue Cr-**soc**-MOF-1 with a BET surface area of 4549 $m^2\ g^{-1}$ and a pore volume of 2.1 $cm^3\ g^{-1}$ is exceptionally stable [85]. It shows a very high water uptake of 200 wt% at 70% relative humidity over more than 100 adsorption/desorption cycles. Such high capacity would make it ideal in potential applications for humidity control in confined spaces and as a dehumidifying material.

If trigonal prismatic $Fe_3O(–COO)_6$ SBUs (D_{3h}) are linked with perfectly square-shaped TCPP (D_{4h}, H_4TCPP = tetrakis(4-carboxyphenyl)porphyrin) $Fe_3O(TCPP)_{3/2}$, PCN-600, is produced (Fig. 9) [86]. The synthesis was carried out following a previously described kinetically tuned dimensional augmentation method, using a preformed $Fe_3O(OAc)_6$ (HOAc = actetic acid) [87]. PCN-600 exhibits a binodal (4,6)-c **stp** topology and has one type of channel with a large diameter of 31 Å. Gas adsorption measurements on the metalated variant PCN-600(Fe) using N_2 at 77 K revealed a type IV isotherm, suggesting mesoporosity, with an apparent BET surface area of 2270 $m^2\ g^{-1}$ and a pore volume of 1.80 $cm^3\ g^{-1}$. Moreover, PCN-600 showed excellent chemical stability in aqueous solutions at pH greater than 2 and less than 11. The alignment of the porphyrins along the large hexagonal channels makes PCN-600 a potential enzyme-mimetic catalyst, especially under basic conditions.

Recently, multivariate versions of PCN-600 were synthesized, using different metal cations in the SBU as well as in the porphyrin linker [88]. For the first time the metal spatial arrangement was deciphered in MTV-MOFs, leading to the conclusion that they either form domains or occur well-mixed. One particular MOF composition, $Ni_{2.07}Fe_{0.93}O(TCPP\text{-}Co)_{3/2}$, showed the best conversion rate in the photo-oxidation of 1,5-dihydroxynaphthalene. This study further exemplifies that performance of MTV-MOFs is superior and there are almost endless opportunities for fine-tuning based on established MOF platforms.

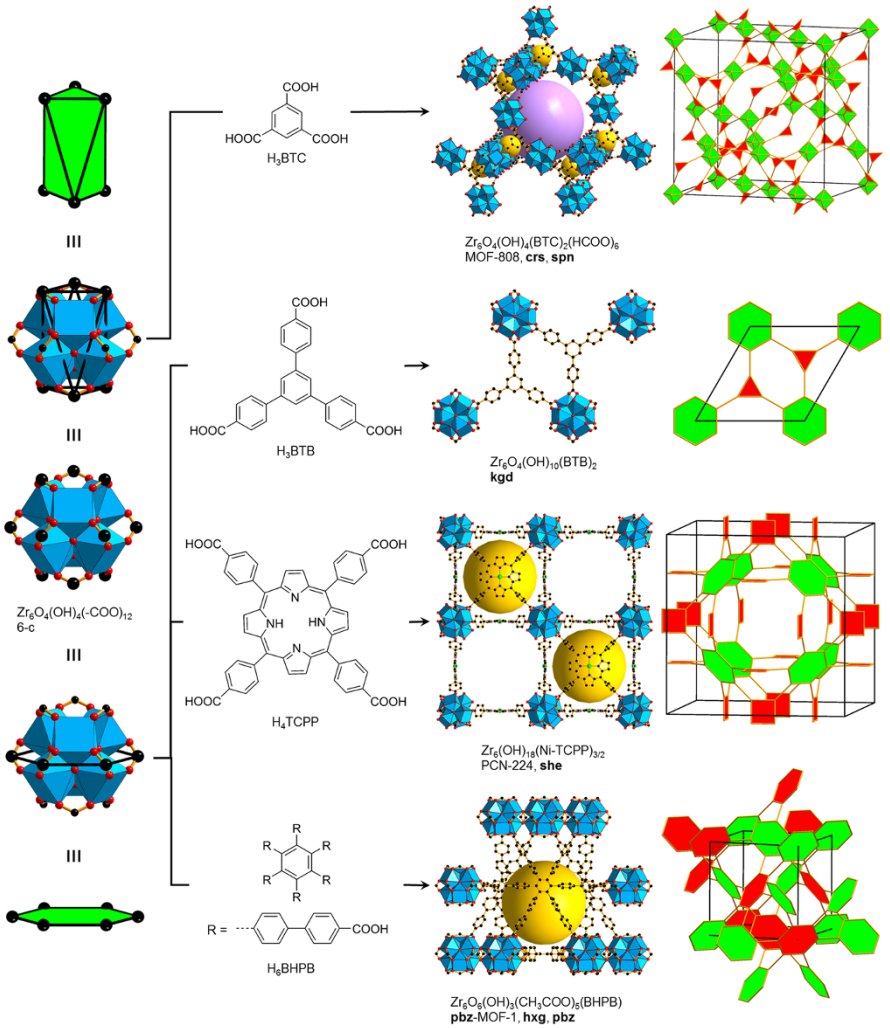

Fig. 10 MOFs constructed from 6-c Zr_6-SBUs. The SBUs are either trigonal antiprismatic or hexagonal planar. Color code: black, C; red, O; green, Ni; blue polyhedra, Zr. The yellow and purple spheres represent the empty space in the framework. Hydrogen atoms are omitted for clarity

6.3 Zirconium Clusters: Trigonal Antiprisms, Hexagonal Planar

Another family of 6-c SBUs is based on zirconium(IV) clusters. Extensive research led to many Zr clusters with different numbers of POE. An early example of a 6-c $Zr_6O_4(OH)_4(–COO)_6$ cluster was observed in MOF-808, $Zr_6O_4(OH)_4(BTC)_2(HCOO)_6$ (Fig. 10) [89]. The 6-c Zr cluster shows a trigonal antiprismatic (D_{3d}) geometry and therefore renders MOF-808 into an overall (3,6)-c **spn** topology. We would like to note here that in the highest symmetry embedding, the 6-c node is an ideal octahedron (O_h). MOF-808 has an internal pore diameter of